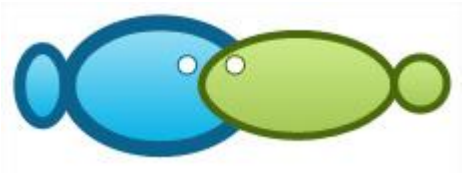

Predicting genetic disorders impacting bone deformities in juvenile hybrid grouper, *Epinephelus fuscoguttatus* X *Epinephelus polyphekadion*: *In silico* interpretation via BMP4, Runx2, and VDR pathways

[1,2]Daniar Kusumawati, [2]Apri I. Supii, [3]Sonny Kristianto, [4]Anita R. P. Raharjeng, [2]Asmanik, [1]Sri Widyarti, [5]Maftuch, [6]Supeno, [1]Sri Rahayu

[1] Biology Department, Faculty of Mathematics and Natural Sciences, Brawijaya University, East Java, Indonesia; [2] Research Center for Marine and Land Bioindustry, National Research and Innovation Agency, Pemenang Barat, Mataram, Indonesia; [3] Forensic Science, Universitas Airlangga, East Java, Indonesia; [4] Biology Department, Faculty of Science and Technology, Universitas Islam Negeri Raden Fatah, Palembang, South Sumatera, Indonesia; [5] Faculty of Fisheries and Marine Science, Brawijaya University, East Java, Indonesia; [6] Faculty of Teacher Training and Education, Wijaya Kusuma University, East Java, Indonesia. Corresponding author: S. Kristianto, sonny.kristianto@pasca.unair.ac.id

Abstract. Understanding the control of bone formation (osteoblast) is crucial for investigating the reasons for bone deformities in *Epinephelus fuscoguttatus* X *Epinephelus polyphekadion* (EFEP) hybrid grouper fry. Proteins, transcription factors, and hormones, such as BMP4, Runx2, and $1.25(OH)_2D3$, interact to control osteoblast formation. BMP4 is a protein that stimulates osteoblast development in conjunction with the transcription factor Runx2. Through binding to the VDR involving Runx2, $1.25(OH)_2D3$ also functions in osteoblast regulation. Malformations of the bone may result from anomalies in the control of bone formation. Mutations in the BMP4, Runx2, and VDR genes can result in regulatory abnormalities. This study aimed to predict the genotypic involvement between parents and offspring in the BMP4, Runx2, and VDR mechanism pathways analyzed by PCR-sequencing and *in silico* 3D protein structure modeling. Bone deformities were known to be induced by mutations in the VDRa gene, as predicted by protein structure modeling. The mutation of a single amino acid sequence alters the structure of the 3D VDRa protein, displacing the attachment location of $1,25(OH)_2D3$, the natural ligand of the VDR. The sequence of amino acids in the Runx2 gene has evolved. The development of this amino acid sequence and its functional influence on the Runx2 protein requires more investigation. Meanwhile, BMP4 has been unable to characterize its involvement in osteoblasts because the primer designed does not adequately describe the protein in the issue. The prediction results indicate that there is involvement of VDRa and Runx2 genetic abnormalities, but more in-depth confirmation of this needs to be carried out with more precise/valid tests.
Key Words: bone malformation, gene mutation, genetic disorder, hybrid grouper.

Introduction. One grouper species exported alive to Hong Kong (Sim et al 2004) is the *Epinephelus fuscoguttatus* X *Epinephelus polypekhadion* hybrid grouper (EFEP), a cross between the female *Epinephelus fuscoguttatus* (tiger grouper) and the male *Epinephelus polyphekadion* (marbled grouper). Therefore, the condition of the fish must conform to export quality criteria, including the absence of disease and normal morphology. High bone deformities, which severely impact the economic worth of fish, pose the greatest obstacle to the production of EFEP. Bone abnormalities also result in sluggish fish growth and high mortality, resulting in substantial operating losses (Koumoundouros et al 2002; Noble et al 2012). There are usually incidences of EFEP deformities in any sea farming operation. From 2014 to 2016, the malformation rate at the Institute of Mariculture Research and Fisheries Extension (IMRAFE) reached 73.4%. Jaw abnormalities, operculum, dorsal saddle

syndrome, underdevelopment of the caudal fin, lordosis, kyphosis, and scoliosis are frequent types of EFEP bone malformations (Ismi et al 2007; Nagano et al 2007; Ebi et al 2018; Iwasaki et al 2018).

The causes of bone abnormalities in farmed fish have been the subject of several investigations. Generally, dietary engineering (Izquierdo et al 2010; Boglino et al 2012) and environmental manipulation are employed to prevent bone deformities (Abdel et al 2004; Georgakopoulou et al 2007; Satoh et al 2008). Mineral deficiencies, such as phosphorus, calcium, vitamin C, DHA, and α-tocopherol, can cause anomalies in bones (Lewis-McCrea & Lall 2010; Fjelldal et al 2012; Izquierdo et al 2013). Environmental variables play an essential role in affecting the correct development of bones in fish embryogenesis, which occurs outside the mother's body (external fertilization). Not only dietary and environmental variables can impact the normal development of fish bones, but also hereditary aspects. The possibility of genetic mutations to arise in their progeny is high because EFEP is a hybrid between two different species. Determining the occurrence of abnormalities based on genetic factors has not been extensively investigated. Therefore, a genetic method will be used in this work to investigate its role in causing bone deformities in EFEP.

Understanding the process of proper bone development (ossification) is crucial for identifying the reasons for physiological bone abnormalities and lowering the prevalence of these conditions. This work focuses on controlling osteoblast formation since malformations in fish bones are present from the larval stage forward. Early bone development begins with the creation of cartilage (chondrocytes), which differentiates into bone (osteoblasts) (Tsumaki et al 2005; Mackie et al 2008). During the development of osteoblasts, various proteins and hormones will interact in a coordinated manner (Datta et al 2008; Bellido et al 2019). The formation of osteoblasts begins with the differentiation of mesenchymal cells into preosteoblasts under the influence of protein interactions, transcription factors, and hormones, such as bone morphogenetic proteins (BMPs), Runx2 transcription factor, and $1.25(OH)_2D3$ (secosteroids, active serum of vitamin D3).

The BMPs are a family of transforming growth factor (TGF) proteins that stimulate bone and cartilage development (Zwijsen et al 2003). By regulating the expression of specific target genes, BMPs are not only engaged in skeletogenesis but also embryogenesis, organogenesis, osteogenesis, cellular differentiation, and apoptosis (Nishimura et al 2003). BMP comprises many types, including BMP-2 through BMP-15 (Cheng et al 2003), each of which has its function. BMP-4 stimulates multipotent mesenchymal cells to differentiate into osteochondrogenic lineage cells and osteoblast progenitor cells (Canalis et al 2003). Smad as a transcriptional factor mediates the effect of BMPs on target cells. Smad stimulates cytoplasm-to-nucleus signal transduction processes and regulates the transcription of target genes with specific binding sites or with the assistance of other transcription factors such as Runx2 (Nishimura et al 2003). Runx2 is a multifunctional transcription factor that plays a crucial role in regulating the expression of extracellular matrix protein genes during osteoblast development (Komori 2010; Carbonare et al 2012; Liu & Lee 2013; Gomathi et al 2020). Runx2 controls the expression of bone matrix genes such as Spp1, Ibsp, and Bglap2, as well as Sp7, osteocalcin, a protein required for osteoblast formation (Liu & Lee 2013; Komori 2017), through binds to promoter osteoblast-specific element 2 (OSE2) (Ducy et al 1997). Runx2 regulates the expression of crucial genes encoding bone matrix proteins, leads pluripotent mesenchymal cells to the osteoblast lineage, and maintains immature osteoblasts. Runx2 and BMP4 are also known to interact with the vitamin D receptor (VDR), and it has been demonstrated that inhibiting VDR expression with VDR siRNA downregulates the expression of Runx (Cbfa1) and BMP-2 (Li et al 2009). Through the crosstalk pathway, BMP4 and VDR stimulate osteoblast development (Figure 1).

This study focused primarily on predicting the genetic factors to determine the causes of deformities in EFEP. It is suspected that an abnormality in the bone formation pathway involving crosstalk between the BMP4, Runx2, and VDR genes can lead to aberrant bone development. This study aimed to predict the variations in the BMP4.

Predicting genetic disorders in bone deformities is indeed crucial for various reasons. Firstly, it allows early detection and intervention, potentially mitigating the severity of the

deformity or preventing it altogether. Secondly, understanding the genetic basis of bone deformities can provide insights into underlying mechanisms, aiding in the development of targeted therapies or management strategies. Lastly, such predictions can inform breeding practices in aquaculture, promoting the selection of healthier and more robust stocks.

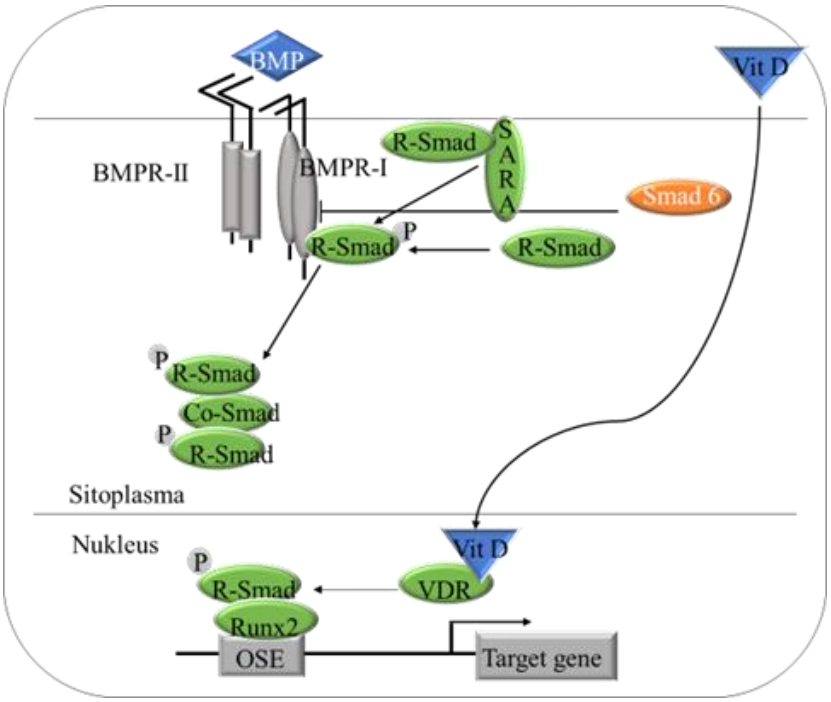

Figure 1. Cross-talk between BMP, Runx2, and vitamin D is essential in osteoblast differentiation control. Smad is responsible for regulating BMP as a ligand. R-Smad is a Smad-regulating receptor with MH1 and MH2 active site domains that, in an inactive state, bind to SARA (Smad-anchor for receptor activation). BMP binds to BMPR II and BMPR I to activate R-Smad (Smad 1, Smad 5, Smad 8), and this activation induces R-Smad association with Co-Smad (Common-partner Smad). The R-Smad and Co-Smad (Smad 4) heterocomplexes subsequently translocate to the nucleus, influencing the transcription of target genes. The Smad heterocomplex can bind with the Runx2 transcription factor and other transcription factors to activate target genes. The vitamin D receptor complex (VDR) and its natural ligand $1.25(OH)_2D3$ interact with the transcription factor Runx2 to facilitate osteoblast regulation. $1,25(OH)_2D3$ is an active serum produced from the conversion of vitamin D3 by the 1-Hydroxylase enzyme.

In summary, the prediction of genetic disorders in bone deformities is paramount for early intervention, personalized treatment, breeding programs, and advancing scientific understanding, all of which are essential for improving the health and welfare of affected individuals, Runx2, and VDR gene sequences in EFEP grouper fingerlings with skeletal deformities. The purpose of this work was to examine the genotypic involvement of parents and offspring in the BMP4, Runx2, and VDR mechanism pathways using PCR-sequencing and in silico 3D protein structure estimation.

Material and Method

Research object. The object of research were 35-day-old juveniles EFEP and its parents. The EFEP is the outcome of interbreeding (hybridization) between a female tiger grouper (*Epinephelus fuscoguttatus*) and a male marble grouper (*Epinephelus polyphekadion*). The broodstock sample consisted of fins, while the 35-day-old (D35) juvenile samples consisted of the body (flesh muscle). Juveniles were euthanized during sample collection by immersion in 20 ppm clove oil (Kizak et al 2013). To collect the fin samples from the broodstock, the fish were first anesthetized for 120 seconds with 40 ppm phenoxyethanol (Kizak et al 2013). The selection of juveniles for sampling was based on normal and

abnormal architecture. Larvae were reared in a controlled environment at the Institute for Mariculture Research and Fisheries Extension (IMRAFE).

PCR sequencing. Female tiger grouper (Ef), male marble grouper (Ep), normal juveniles (EFEP N), and malformed juveniles (EFEP C) were employed in the PCR sequencing assay. In this study, all offspring originated from the same pair of parents. Ten juveniles per pool per tank were collected. There were three replications in treatments, so the total sample was collected at 30 individuals. All samples were isolated from DNA using the FavorPrep genomic DNA extraction mini kit (Favorgen Biotech Corp. Taiwan) technique. A 100 bp DNA ladder from Promega (USA) was used for the amplified marker. The sequences of *Epinephelus coioides* (FJ436409.1), *Takifugu rubripes* (NM 001032643.2), *Dicentrachus labrax* (AM040727.1), *Dicentrachus labrax* (AM040728.1), and *Sparus auratus* (AF289506.1) were used to create the primers BMP4, Runx2, VDRa, and VDRb (Table 1). Primers were designed using PerlPrimer software version 1.121 and Serial Cloner version 2.6.1. PCR was conducted using 2x go tag green (Promega) based on the optimization of each primer (Table 1). Analysis of the PCR-DNA product was followed by sequencing. Multiple sequence alignment (MAFFT alignment) software was used to assess the sequencing findings (Katoh & Standley 2013).

Table 1

Primer design and PCR-DNA optimization

No	*Gene*		*Sequences*	*PCR*		
1	*BMP4*	F:	CCAGAGGGAAGGGACATTCC	Denaturation	95	60 s
		R:	CCCTCCTGGTTACCTTTGG	Annealing	57	30 s
				Extension	72	60 s
2	*Runx2*	F:	CTC ACT ACC ACA CCT ACC T	Denaturation	95	60 s
		R:	TCC AGA CAG CTT CAT CCA	Annealing	55	30 s
				Extension	72	60 s
3	*VDRa*	F:	TTT ATT CCA TCC TCT GTT GCA GTC	Denaturation	95	60 s
		R:	TTA GTT TCT GTT GTG GCT GG	Annealing	59	30 s
				Extension	72	60 s
4	*VDRb*	F:	ATC CAG AAT CTG ACT ACA TCC A	Denaturation	95	60 s
		R:	GAA CTT CAA CAA CCT GCT G	Annealing	59	30 s
				Extension	72	60 s

Homology and 3D modeling of protein structure. Sequence consensus was determined using BioEdit to examine DNA sequencing findings. The ExPASy translate software converts DNA sequences into CDS and amino acids. The predicted amino acid sequence was then compared with pblast to assess its similarities to proteins verified at NCBI using the UniProtKB/SwissProt or Protein Data Bank databases (PDB). The Swiss Model was used to evaluate protein homology when the similarity was more than 40%. The Ab-initio approach was conducted if the homology was less than 40% using the web program https://robetta.bakerlab.org/.

Docking protein. Protein docking simulations predicted the interaction between ligands and receptor proteins. Protein docking was performed using Pyrx software, followed by the Pymol and Discovery Studio Visualizer tools to display protein-ligand interactions.

Results

PCR sequencing – conversion of protein sequence. The PCR-DNA amplification values for the BMP4, Runx2, VDRa, and VDRb genes in the female parental tiger grouper, male parental marble grouper, and their progeny were 100 bp, 200 bp, 500 bp, and 200 bp, respectively (Figure 2). Findings from PCR-DNA sequencing of the BMP4 gene showed a range of 211 to 217 bp (Figure 3A), which were then used to generate amino acid sequences (Figure 3B). According to the findings of the DNA sequence alignment, it was

known that there was one sample, EFEP N2, that has seven distinct sequences compared to the other two parental and progeny samples. Fortunately, these seven sequences were not part of the sequence of nucleotide bases that could be translated into amino acids. Except for EFEP C1 and EFEP C2, all samples had identical amino acid sequences. EFEP C1 and EFEP C2 samples had a gap of one amino acid sequence at the end position (Figure 3B). The amino acid sequence prediction findings for the BMP4 protein were restricted, consisting of only 7-8 sequences, such that when homology was performed with pblast, the results were not as predicted. According to pblsat analysis, the amino acid sequences of BMP4 in both parents and all of their offspring were identical, with a 100% query coverage and a maximum score of 28.6 for the amino acid sequences of PilT/PilU family type 4a pilus ATPase from the species *Candidatus kuenenia stuttgartiensis* (Accession WP 164995455. 1). Genetic traits at the BMP4 locus were less able to represent the characteristics of both parents and offspring because there are only a few predictable amino acid targets, so that when a similarity test is performed, the protein in issue is not represented.

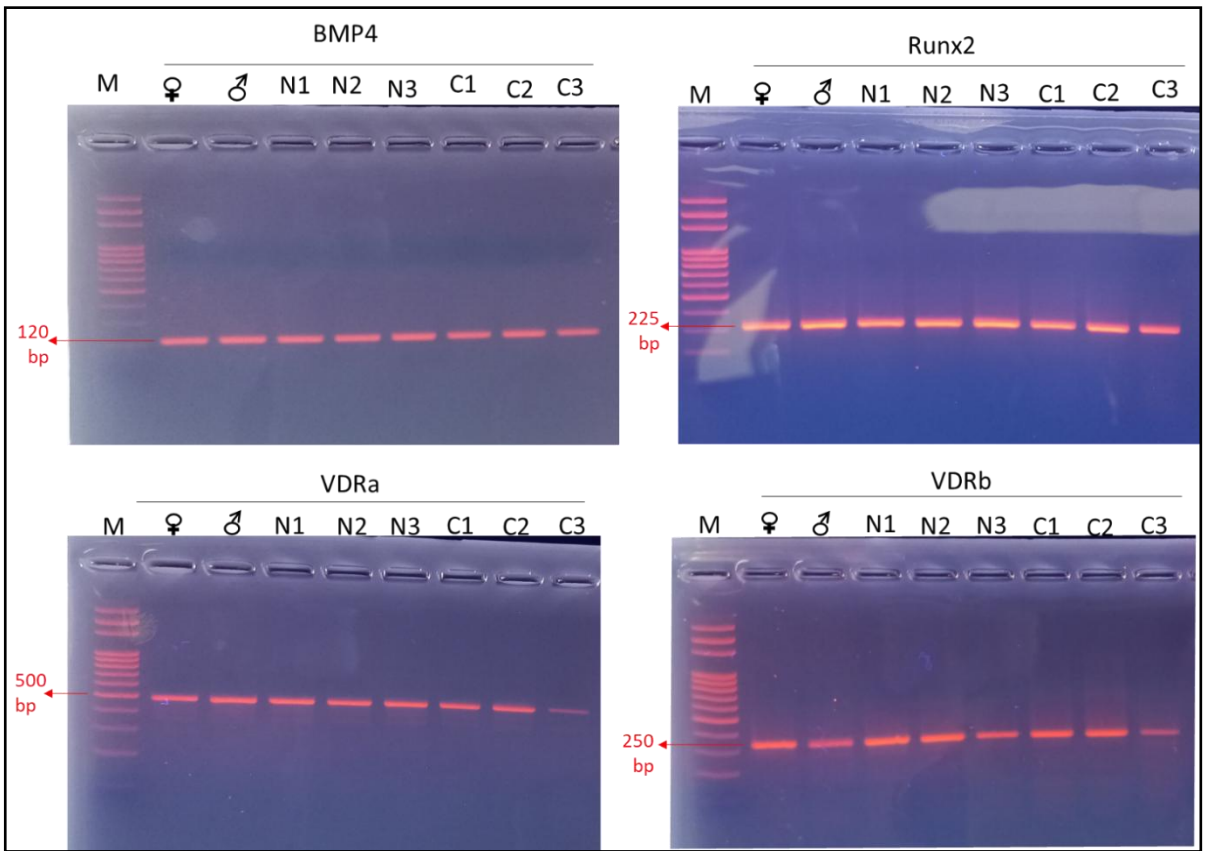

Figure 2. Genes BMP4, Runx2, VDRa, and VDRb were amplified by PCR; M - marker (100 bp); ♀ = female broodstock (*Epinephelus fuscoguttatus*); ♂ = male broodstock (*Epinephelus polyphekadion*); N1–N3 = normal sample; C1–C3 = malformation sample; samples N and C are the descendants of two parents.

PCR-DNA sequencing of the Runx2 gene revealed 267 to 322 base pairs (Figure 4A), which were transformed into amino acid sequences (Figure 4B). According to the results of the DNA sequence alignment, one sample, EfEp N1, contained a nucleotide base (colored blue) that was different from the two parental and other samples. Several gaps exist in the progeny DNA sequences (EFEP N1-N2, EFEP C1-C2) between the two parental sequences (yellow). This provides varied amino acid conversion in the offspring. EFEP N1-N2 and EFEP C2 have identical amino acid sequences to the Ep. The EFEP C1 sample contained amino acid sequences from the female tiger grouper and the male marble grouper, with 19 additional amino acid sequences inserted at sites 81 to 109 (Figure 4B).

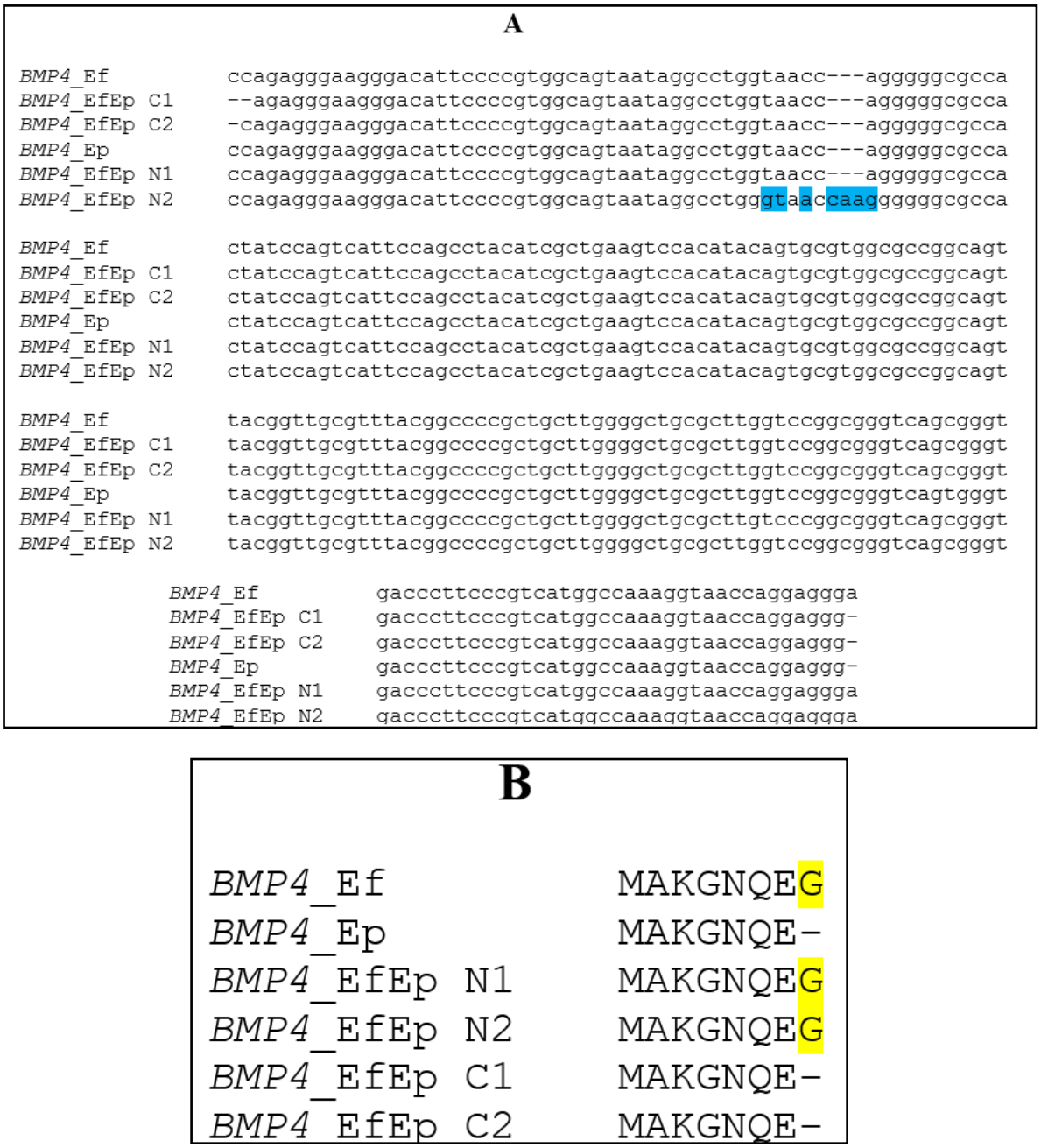

Figure 3. Parental-offspring DNA sequence alignment (A) and BMP4 protein amino acid sequence (B) prediction. The blue color represents a generational sequence distinct from the other parental and offspring patterns. The yellow color indicates a parental and several offspring with the same sequence. The dashed line (-) indicates a gap between the progeny and parental sequence. Ef - *Epinephelus fuscoguttatus* (female tiger grouper); Ep - *Epinephelus polyphekadion* (male marble grouper); EfEp - *Epinephelus fuscoguttatus* X *Epinephelus polyphekadion*; N - normal performance; C - malformation performance (C); 1-2: sample number.

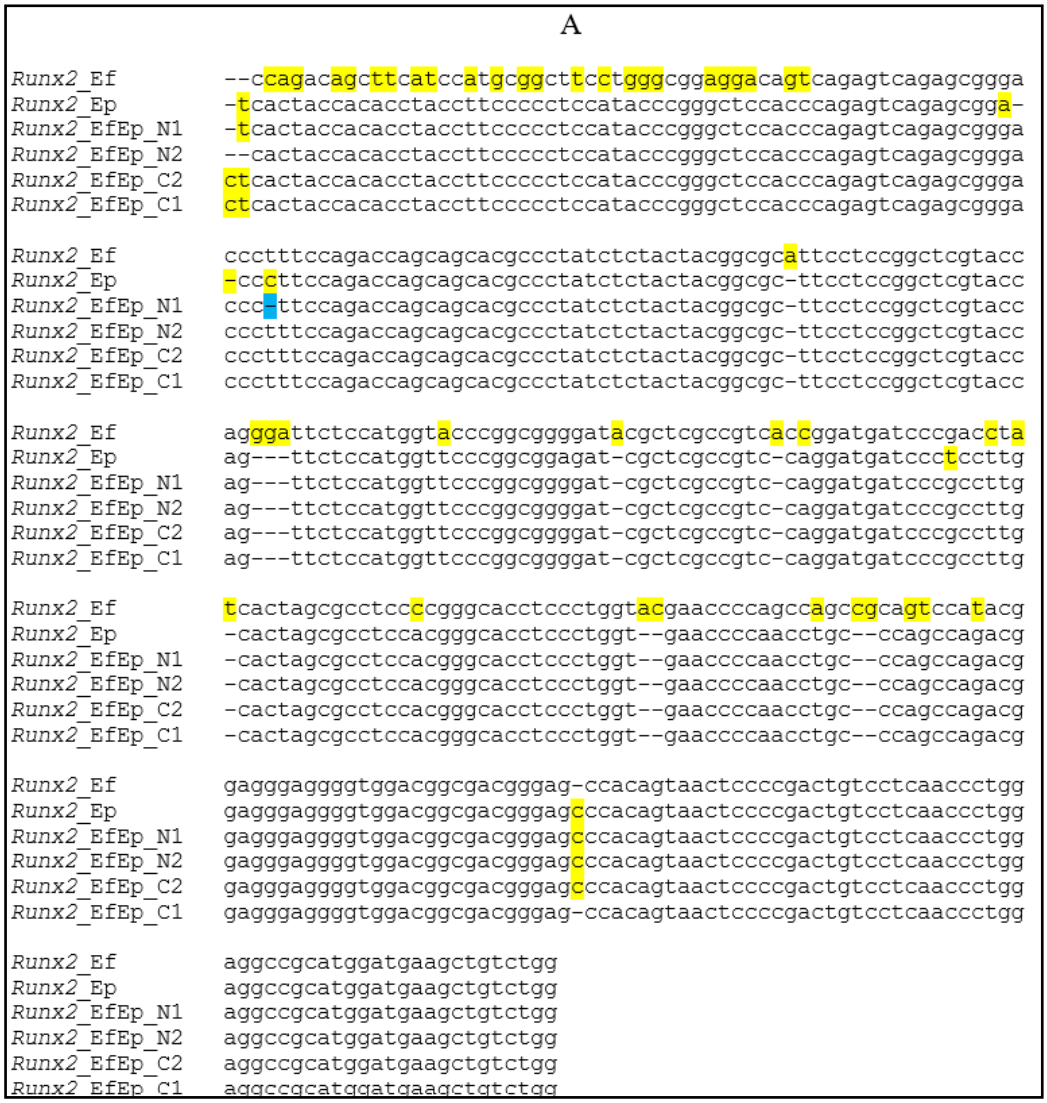

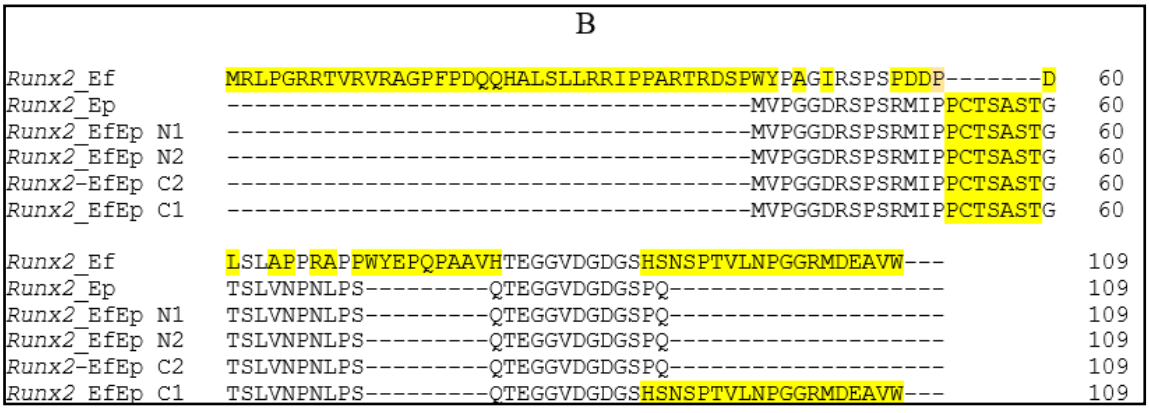

Figure 4. Parental-offspring DNA sequence alignment (A) and Runx2 protein amino acid sequence (B) prediction. The blue color represents a generational sequence distinct from the other parental and offspring patterns. The yellow color indicates a parental and several offspring with the same sequence. The dashed line (-) indicates a gap between the progeny and parental sequence. Ef - *Epinephelus fuscoguttatus* (female tiger grouper); Ep - *Epinephelus polyphekadion* (male marble grouper); EfEp: *Epinephelus fuscoguttatus* X *Epinephelus polyphekadion*; N - normal performance; C - malformation performance (C); 1-2: sample number.

PCR-DNA sequencing of the VDRa gene revealed 668 to 776 base pairs (Figure 5A), which were subsequently transformed into amino acid sequences (Figure 5B). The length of the DNA sequences in the VDRa gene was sufficient to provide a wide range of sequence changes in the mid to late-position progeny sequences that distinguish their parents. The conversion of proteins to DNA sequences obtained 118-140 amino acid sequences (Figure 4B). The amino acid sequences of the progeny EfEp N1-C2 resemble those of Ef except for 14 sequence gaps between positions 1 and 14 and 10 sequence gaps between positions 141 and 150. In all progeny samples, the amino acid sequence at position 94 demonstrated a distinction between their parents A mutation at position 80 in the EFEP C2 was not present in other progeny or parental samples. At that location, the amino acid threonine in EFEP N1-C1 changed into the amino acid methionine in sample C2.

The *VDRb* gene PCR-DNA sequencing results contained 317-325 bp (Figure 6A), which were subsequently converted to amino acid sequences (Figure 6B). Based on the DNA-*VDRb* sequence alignment, all progeny DNA sequences were identical to the parental DNA sequence of Ef (Figure 6A). By converting proteins from DNA sequences, 59 to 61 amino acid sequences were obtained (Figure 6B). According to the amino acid sequence alignment, EfEp N1-N2 and EfEp C1-C2 were 100% homologous with Ef.

Homology of the 3D protein structure. Through the conversion of amino acid sequences in Runx2, all samples were identical to the Mus musculus Runx2 protein (Table 2), the highest homology result according to the UniProtKB2 and Swiss-Prot databases. No proven protein template (PDB) was available for modeling, and 3D structural homology of the Runx2 protein was not allowed. As a result, the ab initio approach was used to generate 3D protein structures. According to the alignment findings with the parental, the EFEP hybrid grouper had two distinct amino acid sequences. The first protein structural model (Figure 7A) was constructed by the sequence of amino acids EfEp N1–N2 and EfEp C2. The second 3D protein structural model (model B) was created based on the amino acid sequence of EfEp C1 (Figure 7B). The insertion of amino acid sequences between positions 81 and 109 in the EfEp C1 sample altered the 3D protein structure modeling (Figure 7B). In all models, the protein structure is dominated by a coil form; however, model A (Figure 7A) contains a helix structure.

All VDRa protein sequences had 3D structural homology with proteins from Rattus novergicus and Homo sapiens in the PDB database. The 3D structural homology was performed using the validated protein structure with the highest sequence identity. Modeling the 3D structure of proteins is strongly connected to their function and role within the biochemical processes of living organisms (Todd, 2003). Thus, the protein's biological mechanism of action may be described based on its three-dimensional structure. The 3D structure of the VDRa protein of the female tiger grouper and male marble grouper was 53.85% similar to the VDR protein structure of Rattus novergicus (PDB accession 3w0h and 5gie) based on the GMQE, QMean, and Ramachandran plot criteria (Table 3). The two samples have 3D structural homology from positions 13 to 61, and 22 amino acid sequences are conserved with the model protein (Figure 8A-B). The EfEp hybrid grouper seeds, both those with normal bone performance (EfEp N1 - N2) and those with malformations (EfEp C1-C2), had homology of 60.53 percent with the 3D protein structure of the Homo sapiens species with the same accession number, 3m7r (Table 3). The two samples had a 3D structural homology from positions 1 to 38, and 23 amino acid sequences were conserved with the model protein (Figure 8C-D).

A


VDRa_Ef
VDRa_Ep
VDRa_EfEp N1
VDRa_EfEp C2
VDRa_EfEp N2
VDRa_EfEp C1

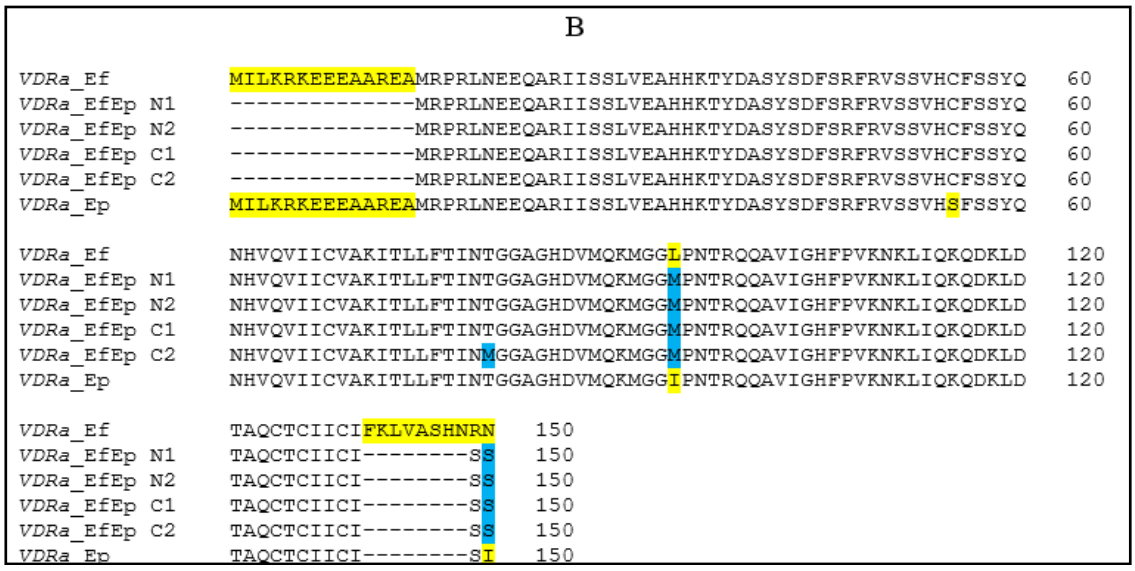

Figure 5. Parental-offspring DNA sequence alignment (A) and *VDRa* protein amino acid sequence (B) prediction. The blue color represents a generational sequence distinct from the other parental and offspring patterns. The yellow color indicates a parental and several offspring with the same sequence. The dashed line (-) indicates a gap between the progeny and parental sequence. Ef - *Epinephelus fuscoguttatus* (female tiger grouper); Ep: *Epinephelus polyphekadion* (male marble grouper); EfEp: *Epinephelus fuscoguttatus* X *Epinephelus polyphekadion* (EFEP hybrid); N - normal performance; C - malformation performance (C); 1-2: sample number.

Considering the homology between parents and offspring, with the template protein remaining low, it is required to model the protein structure using the Ab Initio approach to compare the 3D protein structures of parents and offspring. The first model is a parental sample of a female tiger grouper (Figure 9A), the most comparable to the amino acid sequences of the two offspring. The second model includes three homologous progenies: EFEP N1 - N2 and EFEP C1 (Figure 9B). The third model consists of EFEP C2 with one sequence mutation at position 80 (Figure 9C). According to the 3D protein structure modeling, the protein structure of the parent Ef sample appears to differ significantly from its progeny EFEP N1-N2 and EFEP C1-C2 (Figure 9A). This illustrates the distinction between the 14 sequences at locations 1 to 14 and the ten sequences at locations 141 to 150 in the parent sample Ef. EFEP N1-C1 has a 3D protein structure similar to C2. However, there is a minor difference due to the occurrence of one mutation at position 80, where the amino acid threonine (Thr66) in EFEP N1-C1 is changed to methionine (Met66) in EFEP C2 (Figure 9D).

In all VDRb amino acid sequences, both parents and their offspring with normal and deformities are homologous to the 3D structure of the VDRa protein in *Danio rerio* (PDB accession 3o1e). In all samples, the homology level of protein structure with the protein template is 75% (Table 4). The VDRb protein of all progeny and parental EFEP hybrid grouper contained 22 amino acid sequences, whereas conserved areas with the sequence of the template protein included 21 amino acid sequences (Figure 10 A-B).

Discussion. The presence of bone abnormalities in EFEP could be due to genetic factors. However, not all fish with malformed bones result from a genetic disorder. This was shown by VDRa gene mutation in one sample of the malformed bone progeny (C2), but not in the other samples (C1). This evidence indicates that other variables also contribute to the incidence of bone abnormalities in fish.

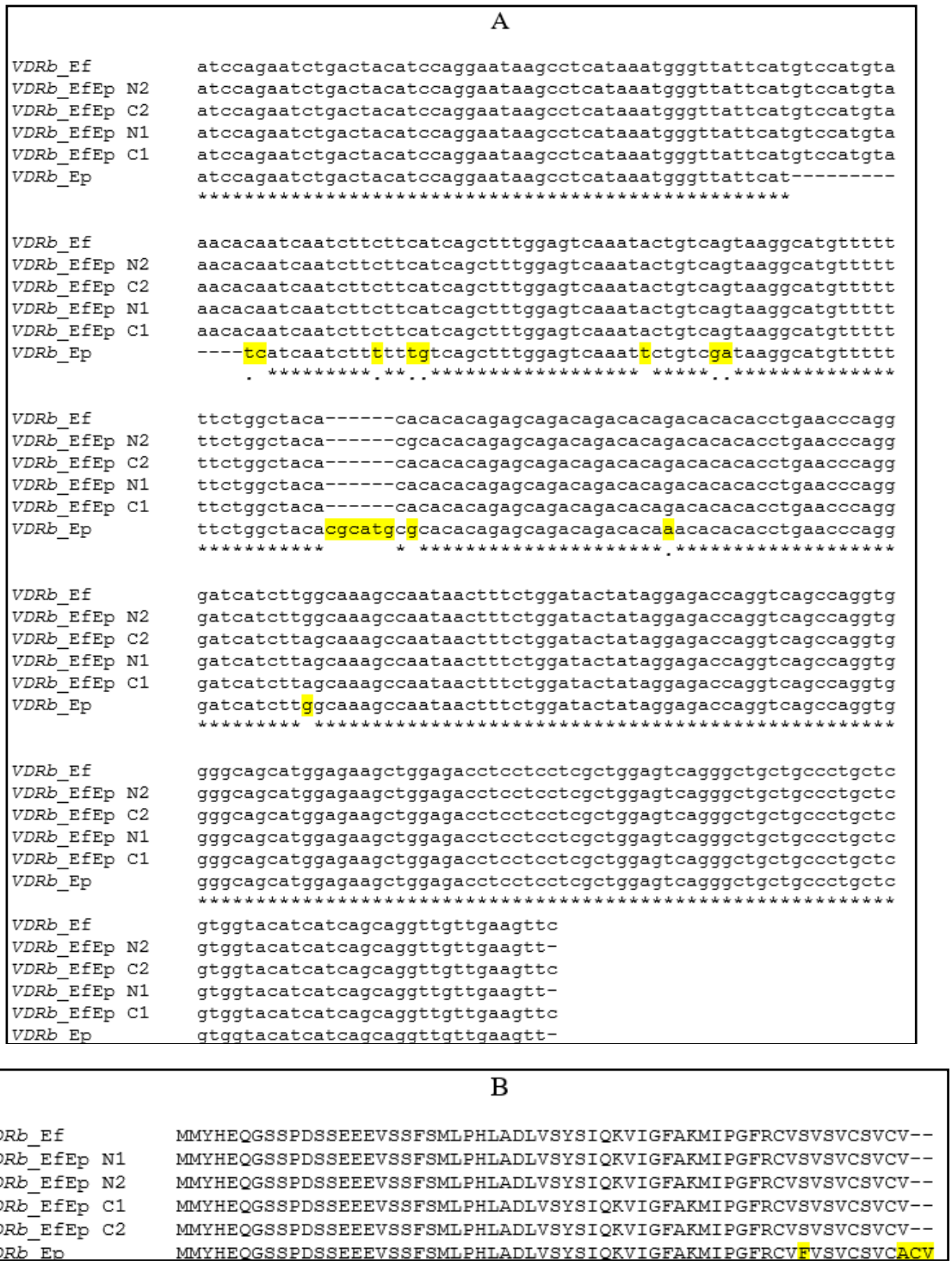

Figure 6. Parental-offspring DNA sequence alignment (A) and *VDRb* protein amino acid sequence (B) prediction. The blue color represents a generational sequence distinct from the other parental and offspring patterns. The yellow color indicates a parental and several offspring with the same sequence. The dashed line (-) indicates a gap between the progeny and parental sequence. Ef - *Epinephelus fuscoguttatus* (female tiger grouper); Ep - *Epinephelus polyphekadion* (male marble grouper); EfEp: *E. fuscoguttatus* X *E. polyphekadion*; N - normal performance; C - malformation performance (C); 1-2: sample number.

Table 2

Runx2 protein homology evaluation based on Swiss-Protein blast results

Code	*Protein sequences quantity*	*Homologous proteins*	*Max score*	*Query cover*	*Percent. identity*	*Description*	*Species*
*Runx2*_Ef	102 AA	Q08775.2	48.9%	25%	80.77%	*Runx2*	*Mus musculus*
*Runx2*_Ep	45 AA	Q08775.2	67.0%	95%	72.09%	*Runx2*	*Mus musculus*
*Runx2*_EfEp N1	45 AA	Q08775.2	67.0%	95%	72.09%	*Runx2*	*Mus musculus*
*Runx2*_EfEp N2	45 AA	Q08775.2	67.0%	95%	72.09%	*Runx2*	*Mus musculus*
*Runx2*_EfEp C1	62 AA	Q08775.2	98.2%	100%	74.19%	*Runx2*	*Mus musculus*
*Runx2*_EfEp C2	45 AA	Q08775.2	67.0%	95%	72.09%	*Runx2*	*Mus musculus*

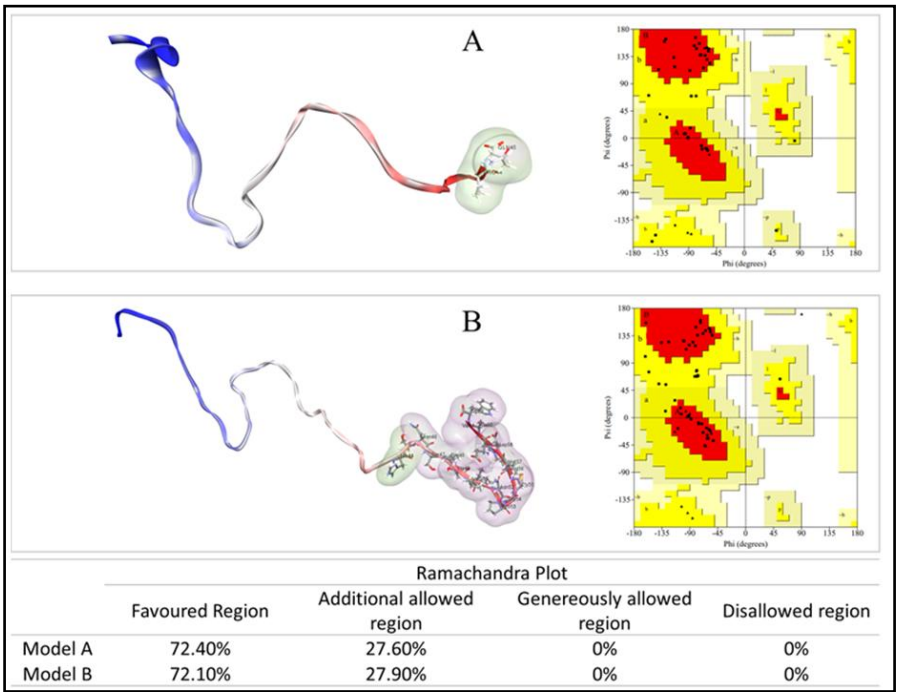

	Ramachandra Plot			
	Favoured Region	Additional allowed region	Genereously allowed region	Disallowed region
Model A	72.40%	27.60%	0%	0%
Model B	72.10%	27.90%	0%	0%

Figure 7. *Runx2* protein modeling via ab initio methods. *Runx2* EfEp N1, N2, and C2 proteins are modeled to be homologous to *Runx2* Ep (male parental gene of marble grouper) (A). *Runx2* C1 protein modeling with 19 proteins inserted at positions 81-109 from the female tiger grouper (B). The color green indicates distinct sequences of amino acids at the precise position. The color red represented a gap in the amino acid sequence of a single protein.

Table 3

Swiss Model-based evaluation of the 3D structural homology of the *VDRa* protein

Code	*Protein Seq. Quantity*	*Protein Template (PDB)*	*Swiss Model*					*Descrip.*	*Species*
			GMQE *	*Qmean* **	*Seq. Ident.*	*Ramach. Favored*	*Ramach. Outlier*		
*VDRa*_Ef	140 AA	3w0h	0.12	0.67	53.85%	97%	0%	*VDR*	*Rattus norvegicus*
*VDRa*_Ep	132 AA	5gie	0.15	0.70	53.85%	100%	0%	*VDR*	*Rattus norvegicus*
*VDRa*_EfEp N1	118 AA	3m7r	0.18	0.71	60.53%	100%	0%	*VDR*	*Homo sapiens*
*VDRa*_EfEp N2	118 AA	3m7r	0.18	0.71	60.53%	100%	0%	*VDR*	*Homo sapiens*
*VDRa*_EfEp C1	118 AA	3m7r	0.18	0.71	60.53%	100%	0%	*VDR*	*Homo sapiens*
*VDRa*_EfEp C2	118 AA	3m7r	0.18	0.71	60.53%	100%	0%	*VDR*	*Homo sapiens*

Note: * - acceptance standards GMQE: 0–1; ** - acceptance standards QMean: 0– -4.

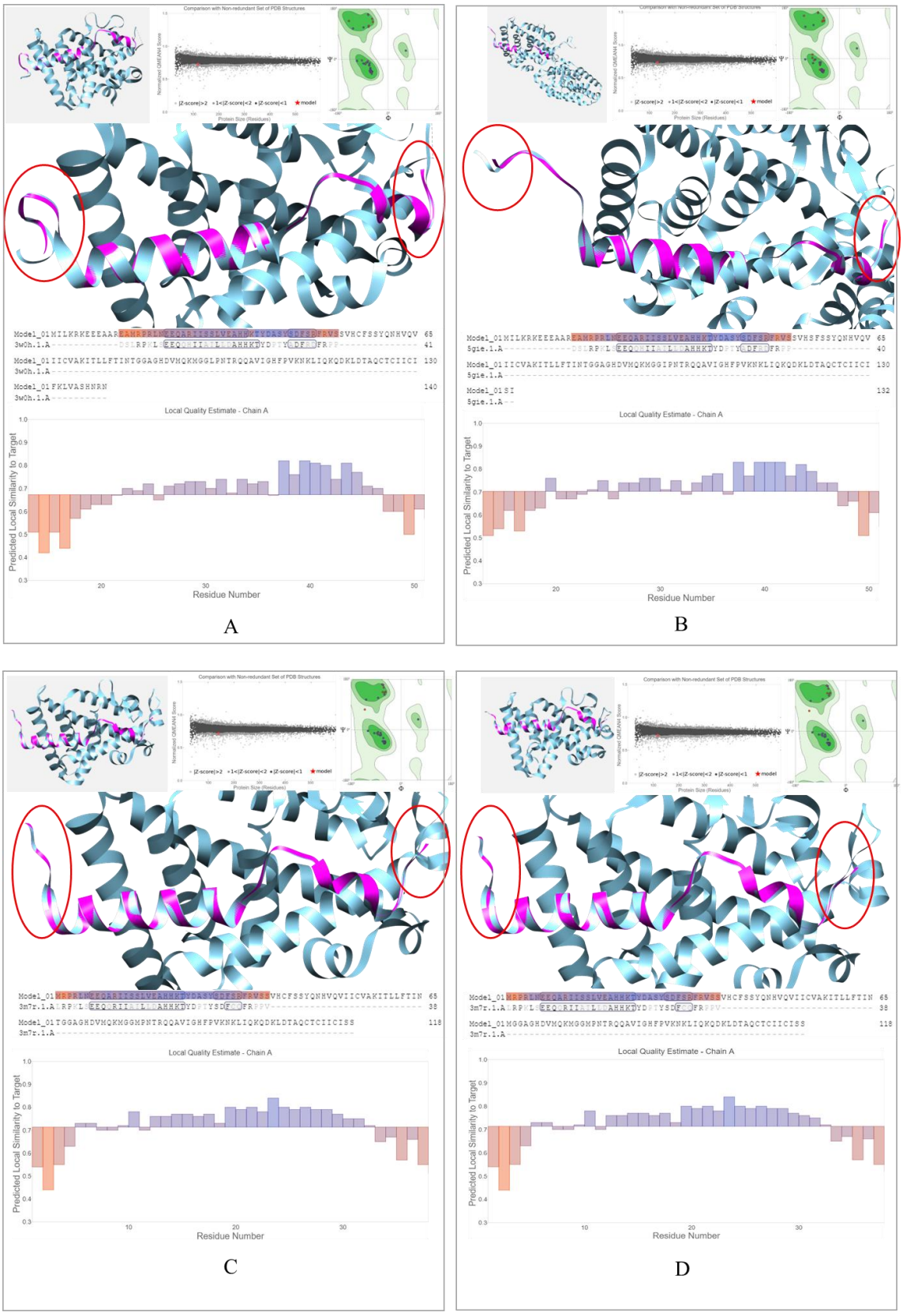

Figure 8. Homology between the three-dimensional structure of VDRa and the protein template. Homology between the VDRa Ef and 3w0h proteins (A). Homology between the VDRa Ep and 5gie proteins (B). Homology between VDRa N1, N2, and C1 and the protein 3m7r (C). Homology between the VDRa C2 and 3m7r (D) proteins.

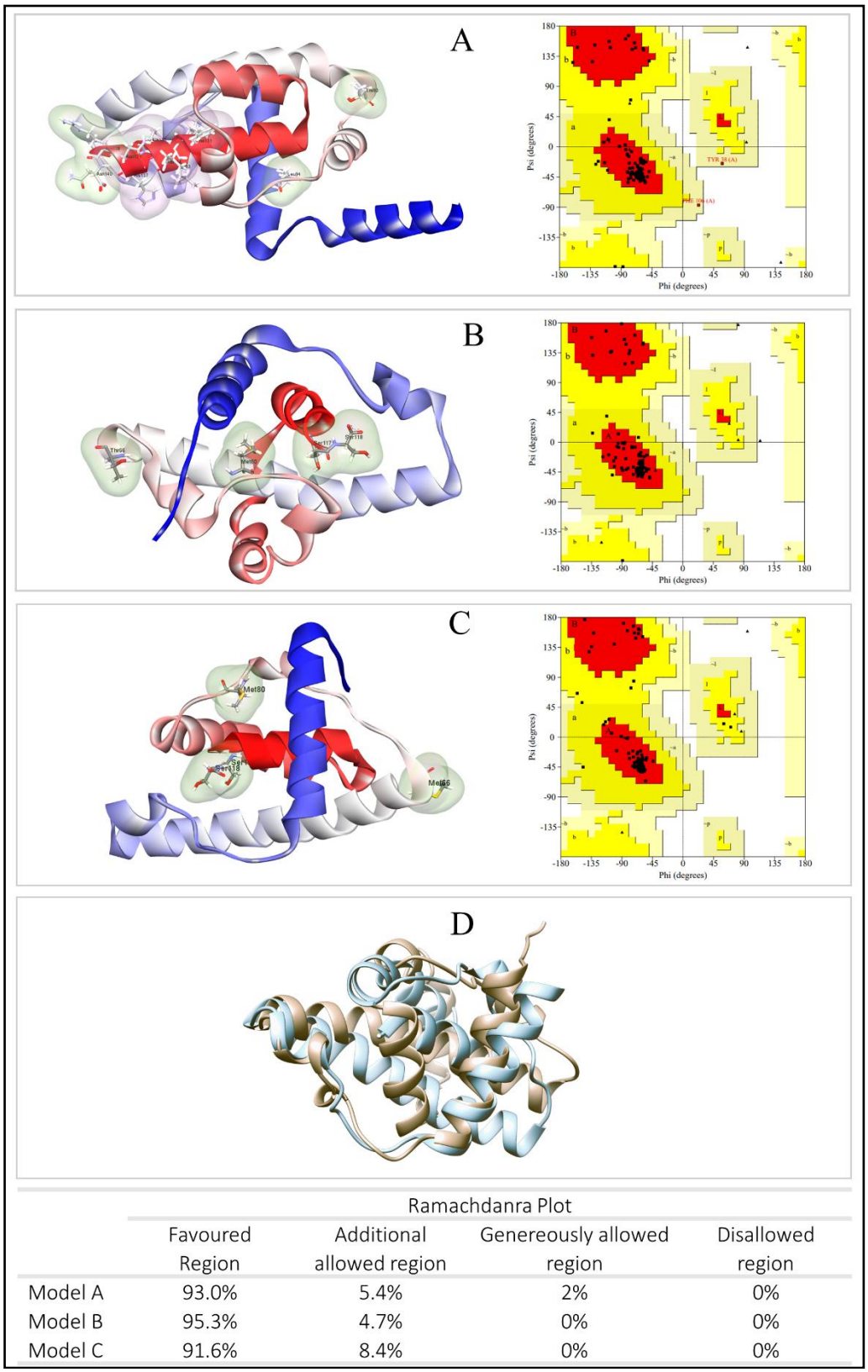

	Ramachdanra Plot			
	Favoured Region	Additional allowed region	Genereously allowed region	Disallowed region
Model A	93.0%	5.4%	2%	0%
Model B	95.3%	4.7%	0%	0%
Model C	91.6%	8.4%	0%	0%

Figure 9. Modeling of VDRa protein using the Ab Initio approach. VDRa Ef protein modeling (parental female tiger grouper) (A); VDRa N1-C1 protein modeling (B); VDRa C2 protein modeling (C); alignment of the VDRa N1 and C2 3D protein structures (D). There was a mutation in VDRa C2 in which the threonine in VDRa N1-C1 (Thr66) and VDRa Ef (Thr80) was replaced by methionine (Met66). Leucine (Leu94) in VDRa Ef has been mutated to methionine (Met94) in VDRa N1-C2 (Met80). The green color indicates different amino acid sequences at the same position. The red color indicates the gap in the amino acid sequence in just one protein.

Table 4

Swiss Model-based evaluation of the 3D structural homology of the *VDRb* protein

Code	Protein seq. quantity	Protein template (PDB)	Swiss Model					Descrip.	Species
			GMQE*	Qmean**	Seq. ident.	Ramach. favored	Ramach. outlier		
*VDRb*_Ef	59 AA	3o1e	0.38	0.9	75%	96.30%	0%	*VDRa*	*Danio rerio*
*VDRb*_Ep	61 AA	3o1e	0.37	0.9	75%	96.30%	0%	*VDRa*	*Danio rerio*
*VDRb*_EfEp N1	59 AA	3o1e	0.37	0.9	75%	96.30%	0%	*VDRa*	*Danio rerio*
*VDRb*_EfEp N2	59 AA	3o1e	0.37	0.9	75%	96.30%	0%	*VDRa*	*Danio rerio*
*VDRb*_EfEp C1	59 AA	3o1e	0.37	0.9	75%	96.30%	0%	*VDRa*	*Danio rerio*
*VDRb*_EfEp C2	59 AA	3o1e	0.37	0.9	75%	96.30%	0%	*VDRa*	*Danio rerio*

Note: * - acceptance standards GMQE: 0–1; ** - acceptance standards QMean: 0– -4.

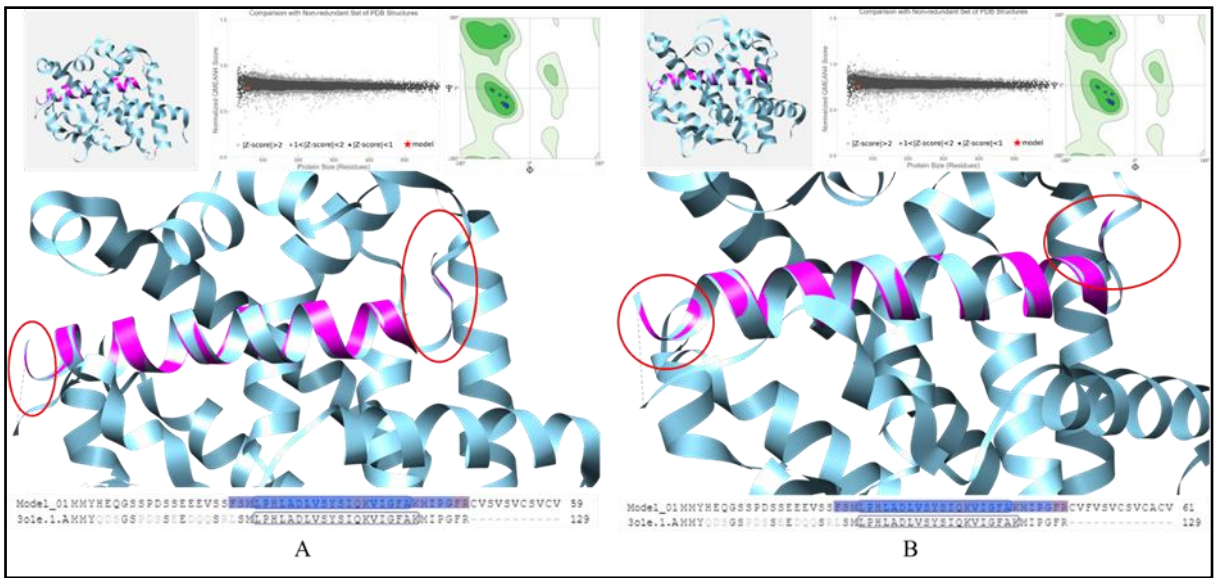

Figure 10. Homology between the three-dimensional structure of the *VDRb* protein and protein template. Homology between the protein structure of *VDRb*-Ef, N1-C2, and the protein template 3o1e (A); homology between the protein structure of *VDRb*-Ep and the protein template 3o1e (B).

At position 80 of the VDRa protein, an amino acid that should be threonine (ACG) is mutated to methionine (ATG). Molecularly, threonine is polar and contains OH (hydroxyl) molecules, whereas methionine is non-polar and contains S (sulfur) molecules (Wayudiadi 2017). This polarity determines how the protein will fold. As a result of their hydrophobic qualities, polar amino acids tend to be located on the exterior of the protein surface in direct contact with water. As a result of their hydrophilic and water-soluble qualities, non-polar amino acids are typically found in the protein fold. The modification of one amino acid affects the 3D protein structure model. One nucleotide base mutation in cytosine (C) that results in thymine (T) alters the 3D model of the protein structure. According to *in silico* prediction analysis, the binding site of the 1,25-dihydroxyvitamin D3 ligand (ChEBI 17823) was not inside the mutation region (Figure 11). Due to structural alterations in the VDRa C2 protein, the location of the ligand attached to the receptor is altered. Manifestations of alterations in protein structure can affect protein functionality (Sotomayor-Vivas et al 2022). However, structural protein alterations are not always accompanied by functional protein disruption. There was a mutation case in 1 amino acid sequence, which did not change the 3D structure of the protein, but this resulted in a decrease in protein function (Dewi 2017). This shows that the mutation site affects the decreasing function of the protein. The mutation site that modifies the structure of the IDCL (interdomain connecting loop) and PIP-binding pocket will impact the binding between the ligand and the protein hence, disrupting protein function (Dewi 2017). Vitamin D receptor (VDR) is a transcription factor that is activated by its natural ligand, 1,25 dihydroxyvitamin D3 (serum active

vitamin D3) (Pike & Meyer 2012). Following activation with its ligands, the VDR complex binds directly to promoter-proximal regions and recruits several coregulatory complexes that influence gene transcription and spread the VD3 genomic activity (Haussler et al 2011; Pike et al 2017). If a mutation occurs in the receptor domain, disruption of the receptor's function in binding to ligands or disruption of the receptor's binding in the promoter region may occur, both of which might impact the production of genes involved in bone growth, thus affecting the regulation of genes involved in bone formation. This suggests that the presence of these mutations causes abnormalities in bone structure, resulting in bone deformities. However, these findings must be confirmed again with more precise tests to prove it.

Evolution of the amino acid sequence can occur spontaneously by cross-breeding between two distinct species, in which the offspring inherit the amino acid configurations of both parents (Lemay & Moineau 2020). This is evident in the malformation (C1) sample from the Runx2 gene, which differs from the other progeny. Manifestations of the insertion of amino acid sequences from both parents result in modifications to the three-dimensional structure of proteins. However, natural evolution may not influence protein functionality due to protein robustness (Tóth-Petróczy & Tawfik 2014). Robustness is associated with the capacity to retain the phenotype despite genotypic alterations (protein biophysics) (Echave & Wilke 2017; Modi et al 2021). Protein robustness is described as the capacity to withstand mutations while retaining the original structure and function, resulting in a series of relatively rapid changes through time (evolution). Thus, changes in the 3D structure of the Runx2 protein may have two alternatives, namely: 1) giving effect; and 2) not having a functional influence in regulating the transcription of the relevant genes. If the evolution of the amino acid sequence in Runx2 has no functional effect, bone production in the BMP4 pathway can be initiated.

Along with Runx2, the BMP4 protein plays a role in the differentiation of progenitor cells into pre-osteoblasts, which regulates the osterix protein (Figure 12). Osterix (Osx) is an osteoblast-specific transcription factor that activates a variety of genes during pre-osteoblast development into mature osteoblasts and osteocytes (Sinha & Zhou 2013). Furthermore, mature osteoblasts will induce the regulation of osteocalcin, which plays a role in bone mineralization (Blair et al 2017; Hosseini et al 2019). Mature osteoblasts are responsible for secreting collagen fiber as a bone matrix and initiating bone mineralization. Mineralization will induce the synthesis of osteocalcin and osteonectin proteins, so that a rigid skeletal framework is formed, but still in the right portion for retaining flexibility. Osteocalcin primarily governs the physical features of bone minerals, such as bone crystal size (Poundarik et al 2018). Osteonectin is responsible for linking the collagen fiber protein to the crystal structure of bone apatite (Zhu et al 2020). Furthermore, osteonectin contributes to the formation of extracellular matrix, including the processing of procollagen and the formation of collagen fibrils, as well as osteoblast differentiation and osteoclast activity (Rosset & Bradshaw 2016).

VD3 performs the same role in activating osterix and its downstream (Figure 12) via the crosstalk route (Han et al 2013; Meyer et al 2014; Ormsby et al 2014; Bruderer et al 2014). VD3 plays a role not only in binding to VDR but also in second messenger pathways that can maintain bone normocalcemia (Boland 2011; Zhu et al 2018). As a result, even if the receptor is functionally compromised due to mutation, VD3 can still play a role in bone mineralization, because Ca ions are the primary ions in the formation of bone crystal matrix during bone mineralization (Chang et al 2000). In this study, genotypic analysis of BMP4 could not accurately represent the qualities of both parents and offspring because the protein targets were not adequately defined. In addition, it is necessary to demonstrate that mutations in VDRa and Runx2 contribute to the incidence of EFEP malformation. In this investigation, not all fish with skeletal abnormalities exhibited genotypic variations. This indicates that both internal and extrinsic factors contribute to the incidence of bone abnormalities. Thus, it is vital to determine what external factors cause bone deformities in EFEP.

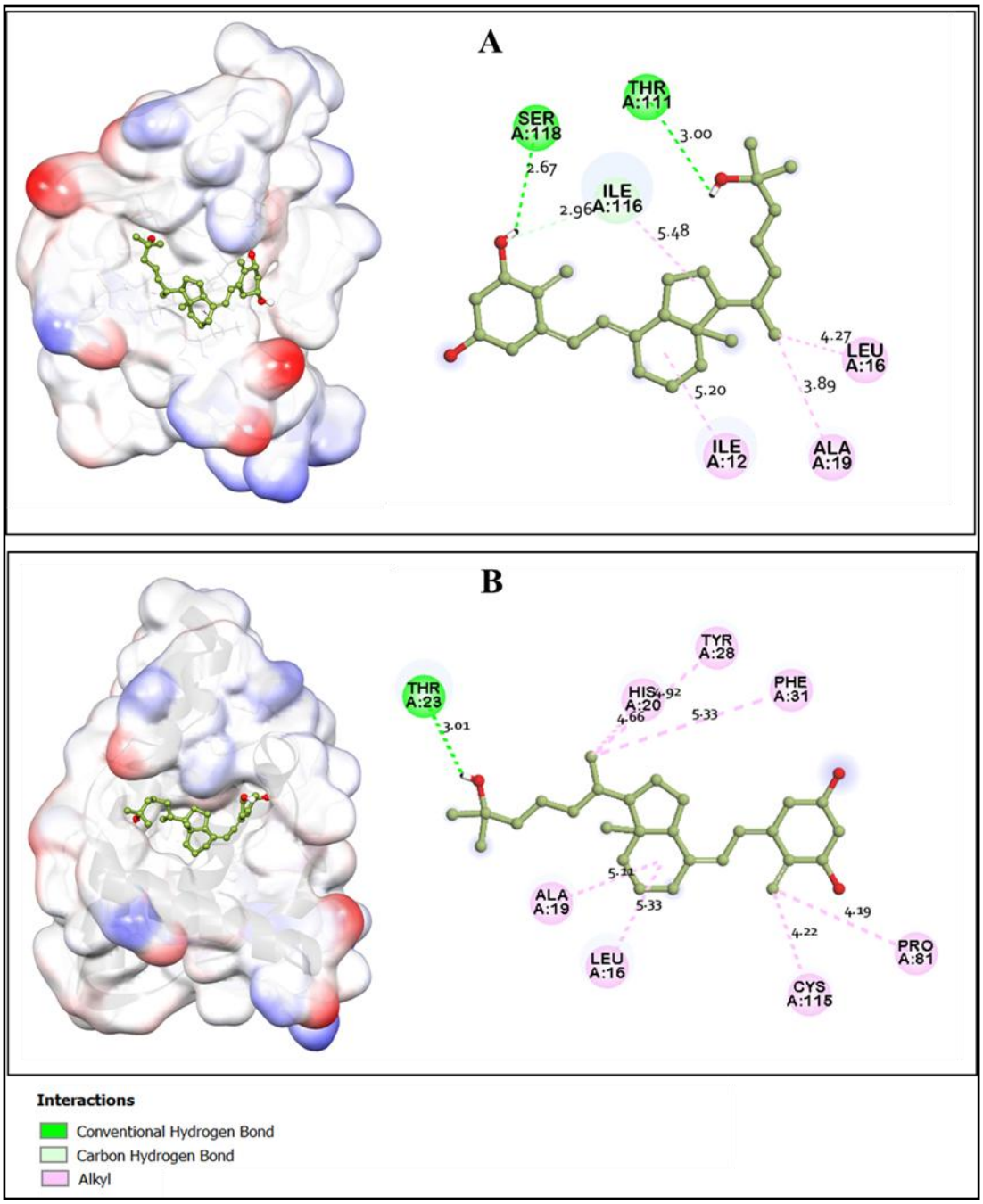

Figure 11. Prediction of the 1.25 dihydroxyvitamin D3 ligand binding to the *VDRa* N1-C1 (A) and *VDRa* C2 receptors (B).

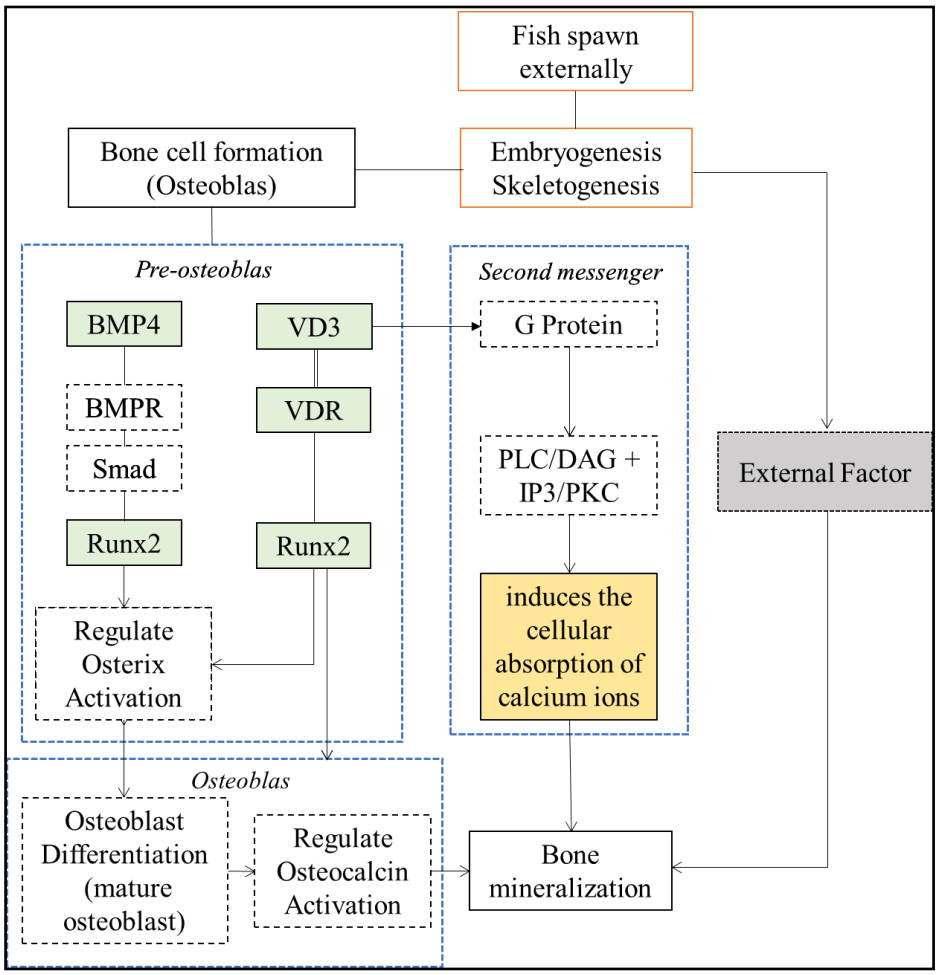

Figure 12. Both hereditary and non-genetic factors are capable of causing the same bone abnormalities. Considering that fish embryogenesis occurs externally, the environment, as an external component, can alter the normal bone regulation process. Through interacting with the transcription factor *Runx2* via the Smad pathway, *BMP4* plays a crucial function in bone regulation. Vitamin D3 (VD3) as a dietary supplement plays a role in bone regulation via second messenger pathways and VDR binding.

Predicting genetic disorders in bone deformities is crucial for various reasons. For instance, it allows for early detection and intervention, potentially mitigating the severity of the deformity or preventing it altogether (Schrodi et al 2014), thus enabling personalized treatment approaches tailored to the specific genetic profile of each affected individual, ultimately optimizing therapeutic outcomes. Additionally, predicting genetic disorders in bone deformities holds significance for breeding programs. The predictions can inform breeding practices in aquaculture, promoting the selection of healthier and more robust stocks (Gjedrem et al 2012). In the case of hybrid grouper, this predictive capability can inform selective breeding programs aimed at reducing the prevalence of these disorders in future generations. Furthermore, it is vital for research advancements. Insights gained from predicting genetic disorders contribute to advancing scientific knowledge of the underlying mechanisms involved in bone development and pathology, thereby leading to the identification of novel therapeutic targets and strategies.

Conclusions. Genetic factors can play a role in bone abnormalities. The occurrence of VDRa mutations and the evolution of the Runx2 gene can disrupt the downstream pathway of bone formation. Nevertheless, VDRa and Runx2 mutations are not the cause of all deformed bones. Based on this, it is reasonable to suspect that external influences also have an essential role in causing bone abnormalities in EFEP. The results of this study

reveal that there is a possibility of involvement of genetic abnormalities in the VDRa and Runx2 pathways. This prediction must be further confirmed with more precise tests. However, this information can be used as a basis for developing therapies to suppress bone abnormalities through nutritional and environmental approaches. As a result, more research into the impact of environmental factors on the occurrence of bone abnormalities is required. In summary, the prediction of genetic disorders in bone deformities is paramount for early intervention, personalized treatment, breeding programs, and advancing scientific understanding, all of which are essential for improving the health and welfare of affected individuals.

Acknowledgements. We never fail to convey our gratitude to the grouper hatchery team at the Institute of Mariculture and Fisheries Extension for their assistance and collaboration.

Conflict of Interest. The authors declare that there is no conflict of interest.

References

Abdel I., Abellán E., López-Albors O., Valdés P., Nortes M. J., García-Alcázar A., 2004 Abnormalities in the juvenile stage of sea bass (*Dicentrarchus labrax* L.) reared at different temperatures: Types, prevalence, and effect on growth. Aquaculture International 12:523-538.

Bellido T., Plotkin L. I., Bruzzaniti A., 2019 Bone cells. In: Basic and applied bone biology. Burr D. B., Allen M. R. (eds), Academic Press, pp. 37-55.

Blair H. C., Larrouture Q. C., Li Y., Lin H., Beer-Stoltz D., Liu L., Tuan R. S., Robinson L. J., Schlesinger P. H., Nelson D. J., 2017 Osteoblast differentiation and bone matrix formation in vivo and in vitro. Tissue Engineering Part B: Reviews 23(3):268-280.

Boglino A., Darias M. J., Ortiz-Delgado J. B., Özcan F., Estévez A., Andree K. B., Hontoria F., Sarasquete C., Gisbert E., 2012 Commercial products for *Artemia* enrichment affect growth performance, digestive system maturation, ossification, and incidence of skeletal deformities in Senegalese sole (*Solea senegalensis*) larvae. Aquaculture 324-325:290-302.

Boland R. L., 2011 VDR activation of intracellular signaling pathways in skeletal muscle. Molecular and Cellular Endocrinology 347(1-2):11-16.

Bruderer M., Richards R. G., Alini M., Stoddart M. J., 2014 Role and regulation of RUNX2 in osteogenesis. European Cells & Materials 28:269-286.

Canalis E., Economides A. N., Gazzerro E., 2003 Bone morphogenetic proteins, their antagonists, and the skeleton. Endocrine Reviews 24(2):218-235.

Carbonare L. D., Innamorati G., Valenti M. T., 2012 Transcription factor Runx2 and its application to bone tissue engineering. Stem Cell Reviews and Reports 8(3):891-897.

Chang Y. L., Stanford C. M., Keller J. C., 2000 Calcium and phosphate supplementation promotes bone cell mineralization: Implications for hydroxyapatite (HA)-enhanced bone formation. Journal of Biomedical Materials Research 52(2):270-278.

Cheng H., Jiang W., Phillips F. M., Haydon R. C., Peng Y., Zhou L., Luu H. H., An N., Breyer B., Vanichakarn P., Szatkowski J. P., 2003 Osteogenic activity of the fourteen types of human bone morphogenetic proteins (BMPs). JBJS 85(8):1544-1552.

Datta H. K., Ng W. F., Walker J. A., Tuck S. P., Varanasi S. S., 2008 The cell biology of bone metabolism. Journal of Clinical Pathology 61(5):577-587.

Dewi S., 2017 [Bioinformatics analysis of the PCNA protein S228i mutation and its effect on the 3-dimensional structure of the protein]. Indonesian Journal of Biotechnology and Biodiversity 1(1):20-27. [In Indonesian].

Ducy P., Zhang R., Geoffroy V., Ridall A. L., Karsenty G., 1997 Osf2/Cbfa1: a transcriptional activator of osteoblast differentiation. Cell 89(5):747-754.

Ebi I., Yong A. S. K., Lim L. S., Shapawi R., 2018 Dietary ascorbic acid requirement for the optimum growth performances and normal skeletal development in juvenile hybrid grouper, *Epinephelus fuscoguttatus* × *Epinephelus lanceolatus*. Journal of King Saud University-Science 30(4):493-499.

Echave J., Wilke C. O., 2017 Biophysical models of protein evolution: understanding the patterns of evolutionary sequence divergence. Annual Review of Biophysics 46:85-103.
Fjelldal P. G., Hansen T., Albrektsen S., 2012 Inadequate phosphorus nutrition in juvenile Atlantic salmon hurts long-term bone health. Aquaculture 334-337:117-123.
Georgakopoulou E., Angelopoulou A., Kaspiris P., Divanach P., Koumoundouros G., 2007 Temperature effects on cranial deformities in European sea bass, *Dicentrarchus labrax* (L.). Journal of Applied Ichthyology 23(1):99-103.
Gjedrem T., Robinson N., Rye M., 2012 The importance of selective breeding in aquaculture to meet future demands for animal protein: A review. Aquaculture 350-353:117-129.
Gomathi K., Akshaya N., Srinaath N., Moorthi A., Selvamurugan N., 2020 Regulation of Runx2 by post-translational modifications in osteoblast differentiation. Life Sciences 245:117389.
Han M. S., Che X., Cho G. H., Park H. R., Lim K. E., Park N. R., Jin J. S., Jung Y. K., Jeong J. H., Lee I. K., Kato S., 2013 Functional cooperation between vitamin D receptor and Runx2 in vitamin D-induced vascular calcification. PLoS ONE 8(12):83584.
Haussler M. R., Jurutka P. W., Mizwicki M., Norman A. W., 2011 Vitamin D receptor (VDR)-mediated actions of 1α,25(OH)$_2$vitamin D$_3$: genomic and non-genomic mechanisms. Best Practice & Research Clinical Endocrinology & Metabolism 25(4):543-559.
Hosseini S., Naderi-Manesh H., Vali H., Eslaminejad M. B., Sayahpour F. A., Sheibani S., Faghihi S., 2019 The contribution of osteocalcin-mimetic peptide enhances osteogenic activity and extracellular matrix mineralization of human osteoblast-like cells. Colloids and Surfaces B: Biointerfaces 173:662-671.
Ismi S., Setiadi E., Wardoyo W., Tridjoko T., 2007 [The effect of using a skimmer on abnormalities in the rearing of duck grouper larvae, *Cromileptes altivelis*]. Jurnal Riset Akuakultur 2(1):1-8. [In Indonesian].
Iwasaki T., Inoue N., Teruya K., Hamasaki K., 2018 Osteological development and deformities in hatchery-reared long tooth grouper (*Epinephelus bruneus*): Vertebral column, dorsal-fin supports, and caudal-fin skeleton. Aquaculture Research 49(10):3245-3257.
Izquierdo M. S., Scolamacchia M., Betancor M., Roo J., Caballero M. J., Terova G., Witten P. E., 2013 Effects of dietary DHA and α-tocopherol on bone development, early mineralization, and oxidative stress in *Sparus aurata* (Linnaeus, 1758) larvae. British Journal of Nutrition 109(10):1796-1805.
Izquierdo M. S., Socorro J., Roo J., 2010 Studies on the appearance of skeletal anomalies in red porgy: effect of culture intensiveness, feeding habits and nutritional quality of live prey. Journal of Applied Ichthyology 26(2):320-326.
Katoh K., Standley D. M., 2013 MAFFT multiple sequence alignment software version 7: improvements in performance and usability. Molecular Biology and Evolution 30(4):772-780.
Kizak V., Guner Y., Kayim M., Can E., 2013 The effects of clove oil on adult males and females of rainbow trouts (*Oncorhynchus mykiss*) and brown trouts (*Salmo trutta fario*). Journal of Food Agriculture and Environment 11(3-4):1542-1545.
Komori T., 2010 Regulation of bone development and extracellular matrix protein genes by RUNX2. Cell and Tissue Research 339:189-195.
Komori T., 2017 Roles of Runx2 in skeletal development. Advances in Experimental Medicine and Biology 962:83-93.
Koumoundouros G., Maingot E., Divanach P., Kentouri M., 2002 Kyphosis in reared sea bass (*Dicentrarchus labrax* L.): ontogeny and effects on mortality. Aquaculture 209(1-4):49-58.
Lemay M. L., Moineau S., 2020 How are genes modified? Crossbreeding, mutagenesis, and CRISPR-Cas9. In: Genetically modified and irradiated food. Andersen V. (ed), Academic Press, pp. 39-54.
Lewis-McCrea L. M., Lall S. P., 2010 Effects of phosphorus and vitamin C deficiency, vitamin A toxicity, and lipid peroxidation on skeletal abnormalities in Atlantic halibut (*Hippoglossus hippoglossus*). Journal of Applied Ichthyology 26(2):334-343.

Li C. J., Gu H. Y., Zhao D. Y., Liu X. M., Zhang X., 2009 Effects of vitamin D receptor interference on the mRNA expression of Dmp1, Cbfa1, and BMP-2 in mouse osteoblast mc3t3-E1 cells. Acta Universitatis Medicinalis Nanjing (Natural Science) 29(5):669-673.
Liu T. M., Lee E. H., 2013 Transcriptional regulatory cascades in Runx2-dependent bone development. Tissue Engineering Part B: Reviews 19(3):254-263.
Mackie E., Ahmed Y. A., Tatarczuch L., Chen K. S., Mirams M., 2008 Endochondral ossification: how cartilage is converted into bone in the developing skeleton. The International Journal of Biochemistry & Cell Biology 40(1):46-62.
Meyer M. B., Benkusky N. A., Lee C. H., Pike J. W., 2014 Genomic determinants of gene regulation by 1,25-dihydroxyvitamin D3 during osteoblast-lineage cell differentiation. Journal of Biological Chemistry 289(28):19539-19554.
Modi T., Campitelli P., Kazan I. C., Ozkan S. B., 2021 Protein folding stability and binding interactions through the lens of evolution: a dynamical perspective. Current Opinion in Structural Biology 66:207-215.
Nagano N., Hozawa A., Fujiki W., Yamada T., Miyaki K., Sakakura Y., Hagiwara A., 2007 Skeletal development and deformities in cultured larval and juvenile seven-band grouper, *Epinephelus septemfasciatus* (Thunberg). Aquaculture Research 38(2):121-130.
Nishimura R., Hata K., Ikeda F., Matsubara T., Yamashita K., Ichida F., Yoneda T., 2003 The role of Smads in BMP signaling. Frontiers in Bioscience 8:s275-s284.
Noble C., Jones H. A. C., Damsgård B., Flood M. J., Midling K. Ø., Roque A., Sæther B. S., Cottee S. Y., 2012 Injuries and deformities in fish: Their potential impacts upon aquacultural production and welfare. Fish Physiology and Biochemistry 38(1):61-83.
Ormsby R. T., Findlay D. M., Kogawa M., Anderson P. H., Morris H. A., Atkins G. J., 2014 Analysis of vitamin D metabolism gene expression in human bone: Evidence for autocrine control of bone remodeling. The Journal of Steroid Biochemistry and Molecular Biology 144:110-113.
Pike J. W., Meyer M. B., 2012 The vitamin D receptor: New paradigms for the regulation of gene expression by 1,25-dihydroxyvitamin D_3. Rheumatic Disease Clinics 38(1):13-27.
Pike J. W., Meyer M. B., Lee S. M., Onal M., Benkusky N. A., 2017 The vitamin D receptor: Contemporary genomic approaches reveal new basic and translational insights. The Journal of Clinical Investigation 127(4):1146-1154.
Poundarik A. A., Boskey A., Gundberg C., Vashishth D., 2018 Biomolecular regulation, composition and nanoarchitecture of bone mineral. Scientific Reports 8(1):1191.
Rosset E. M., Bradshaw A. D., 2016 SPARC/osteonectin in mineralized tissue. Matrix Biology 52:78-87.
Satoh S., Haga Y., Fushimi H., Kotani T., 2008 Effect of zinc and manganese supplementation in *Artemia* on growth and vertebral deformity in red sea bream (*Pagrus major*) larvae. Aquaculture 285(1-4):184-192.
Schrodi S. J., Mukherjee S., Shan Y., Tromp G., Sninsky J. J., Callear A. P., Carter T. C., Ye Z., Haines J. L., Brilliant M. H., Crane P. K., 2014 Genetic-based prediction of disease traits: Prediction is very difficult, especially about the future. Frontiers in Genetics 5:162.
Sim S. Y., Montaldi P., Montaldi A., Kongkeo H., 2004 Grouper farming, market chains, and marine finfish prices in Indonesia. In: Aquaculture Asia Magazine, p. 39.
Sinha K. M., Zhou X., 2013 Genetic and molecular control of osterix in skeletal formation. Journal of Cellular Biochemistry 114(5):975-984.
Sotomayor-Vivas C., Hernández-Lemus E., Dorantes-Gilardi R., 2022 Linking protein structural and functional change to mutation using amino acid networks. PLoS ONE 17(1):261829.
Tóth-Petróczy Á., Tawfik D. S., 2014 The robustness and immovability of protein folds. Current Opinion in Structural Biology 26:131-138.
Tsumaki N., Yoshikawa H., 2005 The role of bone morphogenetic proteins in endochondral bone formation. Cytokine & Growth Factor Reviews 16(3):279-285.
Wayudiadi D., 2017 [Biochemistry]. LEPPIM Mataram, 255 p. [In Indonesian].

Zhu Y. S., Gu Y., Jiang C., Chen L., 2020 Osteonectin regulates the extracellular matrix mineralization of osteoblasts through the P38 signaling pathway. Journal of Cellular Physiology 235(3):2220-2231.
Zhu Y. W., Wen J., Jiang X. X., Wang W. C., Yang L., 2018 A high calcium-to-phosphorus ratio impairs growth and bone mineralization in Pekin ducklings. Poultry Science 97(4):1163-1169.
Zwijsen A., Verschueren K., Huylebroeck D., 2003 New intracellular components of bone morphogenetic protein/Smad signaling cascades. FEBS Letters 546(1):133-139.
*** https://robetta.bakerlab.org/

Received: 16 June 2024. Accepted: 15 September 2024. Published online: 29 April 2025.
Authors:
Daniar Kusumawati, Research Center for Marine and Land Bioindustry, National Research and Innovation Agency, Pemenang Barat, 83352 Lombok Utara, NTB, Indonesia, e-mail: daniar.kusumawati@brin.go.id
Apri Imam Supii, Research Center for Marine and Land Bioindustry, National Research and Innovation Agency, Pemenang Barat, 83352 Kabupaten Lombok Utara, NTB, Indonesia, e-mail: apri021@brin.go.id
Sonny Kristianto, Forensic Science, Universitas Airlangga, Kampus-B, Sekolah Pascasarjana, Jl. Airlangga 4-6, 60286 Surabaya, East Java, Indonesia, e-mail: sonny.kristianto@pasca.unair.ac.id
Anita Restu Puji Raharjeng, Biology Department, Faculty of Science and Technology, Universitas Islam Negeri Raden Fatah, Jl. Prof. K. H. Zainal Abidin Fikri No. Km. 3, RW.05, Pahlawan, Kec. Kemuning, Palembang City, 30126 South Sumatera, Indonesia, e-mail: anitaraharjeng_uin@radenfatah.ac.id
Asmanik, Research Center for Marine and Land Bioindustry, National Research and Innovation Agency, Pemenang Barat, 83352 Lombok Utara, NTB, Indonesia, e-mail: asma007@brin.go.id
Sri Widyarti, Biology Department, Faculty of Mathematics and Natural Sciences, Brawijaya University, Jl. Veteran No.10-11, Ketawanggede, Kec. Lowokwaru, Malang City, 65145 East Java, Indonesia, e-mail: swid@ub.ac.id
Maftuch, Faculty of Fisheries and Marine Science, Brawijaya University, Jl. Veteran No. 10-11, Ketawanggede, Kec. Lowokwaru, Malang City, 65145 East Java, Indonesia, e-mail: maftuch@ub.ac.id
Supeno, Faculty of Teacher Training and Education, Wijaya Kusuma University, 60225 Surabaya, East Java, Indonesia, e-mail: Bana.supeno@gmail.com
Sri Rahayu, Biology Department, Faculty of Mathematics and Natural Sciences, Brawijaya University, Jl. Veteran No. 10-11, Ketawanggede, Kec. Lowokwaru, Malang City, 65145 East Java, Indonesia, e-mail: srahayu@ub.ac.id

How to cite this article:
Kusumawati D., Supii A. I., Kristianto S., Raharjeng A. R. P., Asmanik, Wdiyarti S., Maftuch, Supeno, Rahayu S., 2025 Predicting genetic disorders impacting bone deformities in juvenile hybrid grouper, *Epinephelus fuscoguttatus* X *Epinephelus polyphekadion*: *In silico* interpretation via BMP4, Runx2, and VDR pathways. AACL Bioflux 18(2):1056-1077.